Crack Width Control for Combined Reinforcement of Rebars and Fibres exemplified by Ultra-High-Performance Concrete

Torsten Leutbecher, Ekkehard Fehling

1 Introduction

Concrete shows a low tensile strength in comparison to the compressive strength, which, in addition, grows only under-proportionally with increasing compressive strength. At the same time, the brittleness of the matrix increases. Therefore, especially for Ultra-High-Performance Concrete (UHPC), fibres, usually high-strength steel fibres, are added in not insignificant quantities to improve ductility and to increase the (bending) tensile strength. However, for the economic realisation of wide-span structures under systematic utilisation of the high concrete compressive strength, additional non-prestressed or prestressed reinforcement in the tensile zone is still necessary.

As a result of the interaction of continuous bar reinforcement and distributed short fibres, differences in the load-carrying and deformation behaviour arise in comparison to the well-known reinforced and prestressed concrete. Particularly, stiffness and cracking [Win98, Bal99, Pfy01], but also load-carrying capacity and ductility [Sch06] are considerably affected by the reinforcement configuration. Therefore, the calculation of structures made of UHPC requires models and design procedures, which describe the mechanical procedures under tensile stress appropriately and thus allow a material adequate construction. Thereby, the crack widths play an important role in the serviceability limit state (SLS). If these are limited in sufficient manner (order of magnitude: 50 µm), the protection of the reinforcement from chloride-induced corrosion can then be ensured exclusively by the concrete cover because of the small permeability in the range of finely distributed hair-cracks [Cha04, Brü05].

Habel [Hab04] investigated experimentally the behaviour of a composite consisting of a normal-strength reinforced concrete beam and an UHPC-topping layer applied in the tensile zone. The fibre-reinforced fine-aggregate UHPC (CEMTEC$_{multiscale}$®) showed a fibre content of 6 vol.-%. Fibres with a length of 10 mm and a diameter of 0.2 mm were used. In the UHPC-layer partially an additional bar reinforcement was arranged. In these cases, the bar reinforcement content of the UHPC-topping was 2.0 %. Especially the different crack patterns of the exclusively fibre-reinforced layer on the one hand and of the UHPC-topping additionally strengthened with rebars on the other hand are remarkably. While without bar reinforcement, the crack spacings, which are expected for the pure normal-strength reinforced concrete element, could be observed also in the UHPC-layer (fig. 1.1a), the maximum crack spacing with combined reinforcement was only 30 mm (fig. 1.1b).

As this example clarifies, the crack distribution and thus the crack width can obviously be controlled much more effectively by a combination of fibres and rebars than exclusively by a high fibre content. Besides, experimental investigations in [Leu07] confirm that the fibre-reinforced UHPC does not have to show a hardening behaviour itself in combination with continuous reinforcing elements, in order to obtain an altogether hardening behaviour and thus a distributed cracking with very small crack spacings and crack widths. Rather, relatively small fibre contents of under 1 vol.-% are sufficient. Especially from the ecological view this is very favourable, because the high employment of energy and resources, which is necessary for the production of thin high-strength steel fibres, can be limited. At the same time, a crucial economic advantage is given.

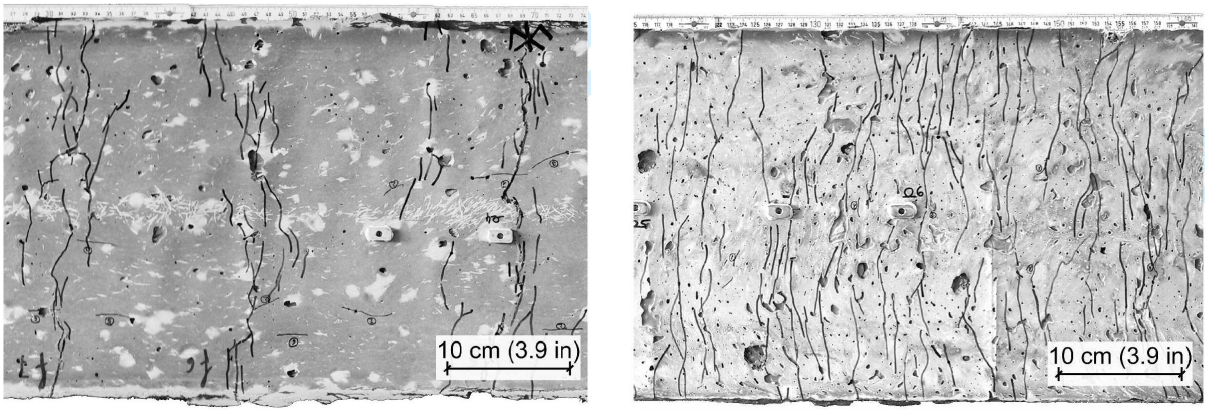

a) b)

Fig 1.1 Crack pattern at ultimate load [Hab07]
a) Exclusively reinforced with steel fibres (6 vol.-%), 3 cm thick UHPC-topping layer
b) Reinforced with steel fibres (6 vol.-%) and rebars (2 %), 5 cm thick UHPC-topping layer

In the following, the mechanical relations, necessary for an analysis of the crack formation process, are derived. For this, in the sections 2 and 3 the performance of the two reinforcing elements ”rebars“ and ”fibres“ firstly are regarded separately from each other. Afterwards, the load-carrying behaviours are linked considering the equilibrium of forces and the compatibility of deformations. Because of their universal formulation, the obtained relationships are generally applicable to all types of concrete reinforced with rebars and fibres, i.e. they are not limited to UHPC.

The load-carrying behaviour and the crack formation within the serviceability range, observed by *Leutbecher* [Leu07] in experimental investigations on combined reinforced tensile members, are also reproduced very well by the presented mechanical model. The material parameters needed for this purpose were determined among others in pull-out-tests and in centric tensile tests on notched fibre-reinforced concrete prisms.

2 Crack Formation of Reinforced Concrete under Short Term Loading

2.1 Single Crack Formation

If the concrete tension stress σ_c reaches the effective matrix tensile strength f_{ct} of the concrete in a weak point of a tensile tie, then a crack forms in the appropriate cross section (fig. 2.1).

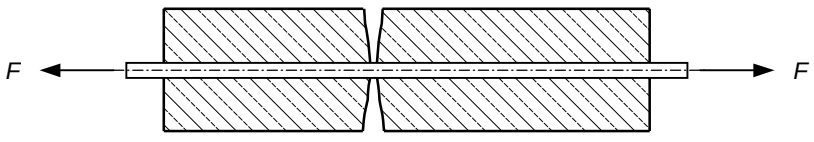

Fig 2.1 First crack of a reinforced concrete tensile tie

The cracking load amounts to

$$F_{cr} = A_c \cdot \left(1+\alpha_E \cdot \rho_s\right) \cdot f_{ct} \tag{2.1}$$

The term $\left(1+\alpha_E \cdot \rho_s\right)$ considers, that, in the uncracked state, the reinforcing bar participates in load bearing in the relationship of its tension stiffness to the total stiffness of the specimen.

In the crack the external tensile load is carried by the reinforcing steel alone. There, the steel tension amounts to

$$\sigma_s = \left(1+\alpha_E \cdot \rho_s\right) \cdot \frac{f_{ct}}{\rho_s} \tag{2.2}$$

In a certain distance of the crack the tensile member is in the uncracked state. A difference between concrete and steel strain thus is present only in parts of the member, within the load transmission length on the left and on the right side of a crack (fig. 2.2).

Hence, the load transmission length l_{es} can be specified for the single crack as follows:

$$l_{es} = \frac{\sigma_s \cdot d_s}{4 \cdot \tau_{sm} \cdot \left(1+\alpha_E \cdot \rho_s\right)} = \frac{f_{ct} \cdot d_s}{4 \cdot \tau_{sm} \cdot \rho_s} \tag{2.3}$$

with σ_s steel stress in the crack
d_s diameter of the bar reinforcement
τ_{sm} average bond stress over the load transmission length

The width of the single crack *w* results from the average difference of steel and concrete strain over the load transmission length l_{es}.

$$w = 2 \cdot l_{es} \cdot \left(\varepsilon_{sm} - \varepsilon_{cm}\right) \tag{2.4}$$

By assumption of a parabolic development of concrete and steel strains (solidity coefficient of about 0.6), the steel and concrete strains averaged over the load transmission lengths, ε_{sm} and ε_{cm}, can be described in good approximation as follows:

$$\varepsilon_{sm} = 0.4 \cdot \varepsilon_s^{II} + 0.6 \cdot \varepsilon_s^{I} \tag{2.5}$$

$$\varepsilon_{cm} = 0.6 \cdot \varepsilon_c^{I} = 0.6 \cdot \varepsilon_s^{I} \tag{2.6}$$

with ε_s^{II} steel strain in the crack
ε_s^{I} steel strain at the end of the load transmission length
ε_c^{I} concrete strain at the end of the load transmission length, $\varepsilon_c^{I} = \varepsilon_s^{I}$

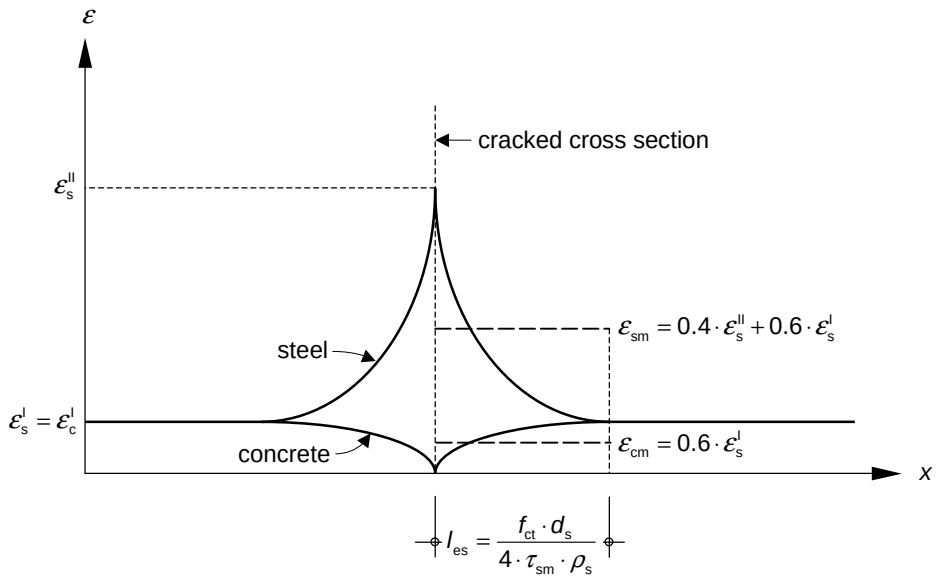

Fig. 2.2 Strains in the state of single crack formation

With equations (2.3) to (2.6), the crack width of the single crack can now be determined as follows:

$$w = \frac{\sigma_s^2 \cdot d_s}{5 \cdot E_s \cdot \tau_{sm} \cdot (1 + \alpha_E \cdot \rho_s)} = \frac{f_{ct}^2 \cdot d_s}{5 \cdot E_s \cdot \tau_{sm} \cdot \rho_s^2} \cdot (1 + \alpha_E \cdot \rho_s) \tag{2.7}$$

Influence of shrinkage

By a modification of the well-known relations presented so far, the influence of shrinkage of the concrete on the crack formation and the crack width development can be considered. This is necessary for a realistic description of the tensile behaviour particularly for UHPC, because of the comparatively high total shrinkage.

Due to shrinkage, the tensile member receives a pre-strain. However, the concrete cannot deform freely because of the restraint exercised by the reinforcement. This leads to tensile stresses in the concrete and compressive stresses in the steel bars (fig. 2.3).

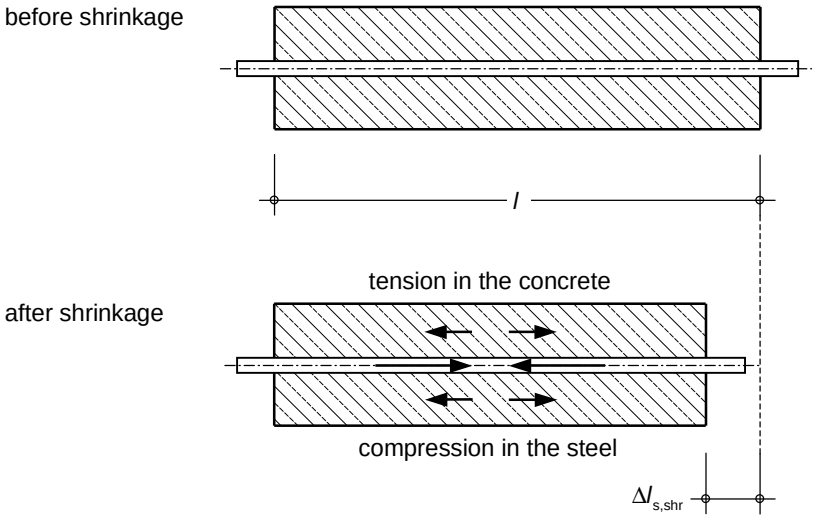

Fig 2.3 Inherent stress condition of a tensile tie due to restraint of shrinkage by the reinforcement

Considering compatibility and equilibrium, the pre-strain due to shortening $\Delta l_{s,shr}$ can be determined for the flexible case according to equation (2.8).

$$\varepsilon_{s,shr}^{el} = \frac{\varepsilon_{cs}}{1 + \alpha_E \cdot \rho_s} \tag{2.8}$$

with ε_{cs} free shrinkage strain of the concrete (shortening = negative value)

If shrinkage and creep run affine to each other, the gradually increasing restraint is partly reduced by relaxation of the concrete. In this case the pre-strain results in

$$\varepsilon_{s,shr} = \frac{\varepsilon_{cs}}{1 + \alpha_E \cdot \rho_s \cdot (1 + \rho \cdot \varphi)} \tag{2.9}$$

with φ creep coefficient at the moment of cracking
ρ relaxation coefficient, may be taken to 0.8 in general

Due to the restraint in the concrete, the external load necessary to produce a single crack is reduced. The cracking force of the tensile member and the steel stress in the crack are thus lower than in the case without shrinkage.

The cracking force under short term loading amounts to

$$F_{cr} = A_c \cdot (1+\alpha_E \cdot \rho_s) \cdot \left(f_{ct} + \varepsilon_{s,shr} \cdot E_s \cdot \rho_s \right) \tag{2.10}$$

The corresponding steel stress in the crack results in

$$\sigma_s = (1+\alpha_E \cdot \rho_s) \cdot \left(\frac{f_{ct}}{\rho_s} + \varepsilon_{s,shr} \cdot E_s \right) \tag{2.11}$$

Directly at the crack surfaces the concrete is now able to shorten freely. This deformation, made possible by omission of the internal restraint, is purely elastic. Therefore, the concrete strain at the crack surface results to

$$\varepsilon^*_{s,shr} = \varepsilon_{s,shr} \cdot (1+\alpha_E \cdot \rho_s) \tag{2.12}$$

Due to relaxation of the concrete during the hardening process until the moment of cracking, the absolute value of the strain according to equation (2.12) is smaller than the absolute value of the free shrinkage coefficient of the concrete. In comparison to the case of pure loading, the strain at the end of the transmission length is reduced by the amount of the pre-strain. The strains are illustrated in fig. 2.4.

Considering the influence of shrinkage, the load transmission length l_{es} results in:

$$l_{es} = \frac{\left(\frac{\sigma_s}{1+\alpha_E \cdot \rho_s} - \varepsilon_{s,shr} \cdot E_s \right) \cdot d_s}{4 \cdot \tau_{sm}} = \frac{f_{ct} \cdot d_s}{4 \cdot \tau_{sm} \cdot \rho_s} \tag{2.13}$$

Thus, the result does not differ from that in the case of pure loading.

The strains of steel and concrete averaged along the load transmission length, ε_{sm} and ε_{cm}, amount to

$$\varepsilon_{sm} = 0.4 \cdot \varepsilon_s^{II} + 0.6 \cdot \varepsilon_s^{I} \tag{2.14}$$

$$\varepsilon_{cm} = 0.4 \cdot \varepsilon^*_{s,shr} + 0.6 \cdot \varepsilon_c^{I} = 0.4 \cdot \varepsilon^*_{s,shr} + 0.6 \cdot \varepsilon_s^{I} \tag{2.15}$$

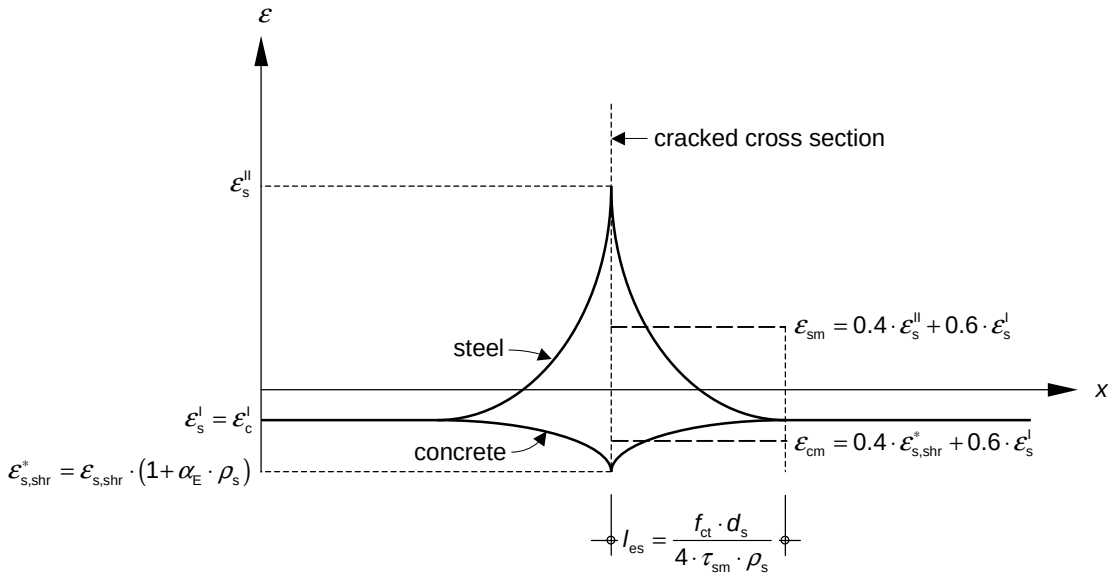

Fig. 2.4 Influence of shrinkage on the strains at the state of single crack formation

With the load transmission length according to equation (2.13) and the average strains ε_{sm} and ε_{cm} according to equations (2.14) and (2.15) the width of a single crack considering shrinkage becomes

$$w = \frac{\left(\frac{\sigma_s}{1+\alpha_E \cdot \rho_s} - \varepsilon_{s,shr} \cdot E_s\right) \cdot d_s}{2 \cdot \tau_{sm}} \cdot \left[0.4 \cdot \varepsilon_s^{II} - 0.4 \cdot \varepsilon_{s,shr}^*\right] \tag{2.16}$$

Inserting equations (2.11) and (2.12) results in

$$w = \frac{\left(\frac{\sigma_s}{1+\alpha_E \cdot \rho_s} - \varepsilon_{s,shr} \cdot E_s\right)^2 \cdot d_s}{5 \cdot E_s \cdot \tau_{sm}} \cdot \left(1+\alpha_E \cdot \rho_s\right) = \frac{f_{ct}^2 \cdot d_s}{5 \cdot E_s \cdot \tau_{sm} \cdot \rho_s^2} \cdot \left(1+\alpha_E \cdot \rho_s\right) \tag{2.17}$$

Thus, in spite of the reduced cracking stress, shrinkage does not influence the width of a single crack.

It can be summarised, that shrinkage causes an internal restraint for reinforced concrete tensile members. Due to this, the cracking load level decreases. However, the load transmission length and the width of a single crack do not differ from the case of pure action of loading without any internal restraint.

Neglecting the concrete strain resulting from the action of loading, the required reinforcement to limit the width of a single crack is obtained directly by transforming the equations (2.7) and (2.17):

$$A_s = \sqrt{\frac{F_s^2 \cdot d_s}{5 \cdot E_s \cdot \tau_{sm} \cdot w_k}} \qquad \text{(without influence of shrinkage)} \tag{2.18}$$

$$A_s = \frac{F_s}{\sqrt{\frac{5 \cdot E_s \cdot \tau_{sm} \cdot w_k}{d_s}} + \varepsilon_{s,shr}^* \cdot E_s} \qquad \text{(considering influence of shrinkage)} \tag{2.19}$$

with F_s tensile force, carried by the reinforcement in the crack
$\varepsilon_{s,shr}^*$ concrete strain at crack surface after crack formation, considering shrinkage and relaxation of concrete; approximately equal to the free shrinkage coefficient of concrete

With the cracking force of the concrete cross section (action of restraint), the required reinforcement arises independently of the amount of shrinkage:

$$A_s = A_c \cdot f_{ct} \cdot \sqrt{\frac{d_s}{5 \cdot E_s \cdot \tau_{sm} \cdot w_k}} \tag{2.20}$$

After the first cracking, new cracks develop due to further load increase within ranges with higher concrete tensile strength. A condition is however that the tensile force, necessary to generate a crack beside an existing crack, is transferred from the steel to the concrete by bond action, i.e. new cracks can appear only outside of the load transmission lengths of the already existing cracks.

2.2 Crack Width and Crack Spacing at Stabilised Cracking

The crack pattern of a structural element changes continuously by cracking, until the force introduced from the steel into the concrete by bond does not reach concrete tensile strength anymore. Then, slip between concrete and reinforcement is present everywhere. This state is characterised as stabilised cracking.

The possible crack spacings s_r measure between the single and the double load transmission length l_{es}.

$$s_{r,min} = l_{es} \le s_r < s_{r,max} = 2 \cdot l_{es} \tag{2.21}$$

with $s_{r,min}$ the smallest possible crack spacing at stabilised cracking
$s_{r,max}$ the largest possible crack spacing at stabilised cracking

For the border case $s_{r,max} = 2 \cdot l_{es}$ the strains at stabilised cracking are depicted in fig. 2.5.

The strains of steel and concrete averaged over the load transmission length, ε_{sm} and ε_{cm}, amount in this case to

$$\varepsilon_{sm} = \varepsilon_s^{II} - 0.6 \cdot \frac{f_{ct}}{\rho_s \cdot E_s} \tag{2.22}$$

$$\varepsilon_{cm} = 0.6 \cdot \frac{f_{ct}}{E_c} = 0.6 \cdot \frac{f_{ct}}{\rho_s \cdot E_s} \cdot \alpha_E \cdot \rho_s \tag{2.23}$$

Therewith, the maximum crack width at stabilised cracking can be determined as follows:

$$w_{max} = s_{r,max} \cdot (\varepsilon_{sm} - \varepsilon_{cm}) = \frac{f_{ct} \cdot d_s}{2 \cdot E_s \cdot \tau_{sm} \cdot \rho_s} \cdot \left[\sigma_s - 0.6 \cdot \frac{f_{ct}}{\rho_s} \cdot (1 + \alpha_E \cdot \rho_s) \right] \tag{2.24}$$

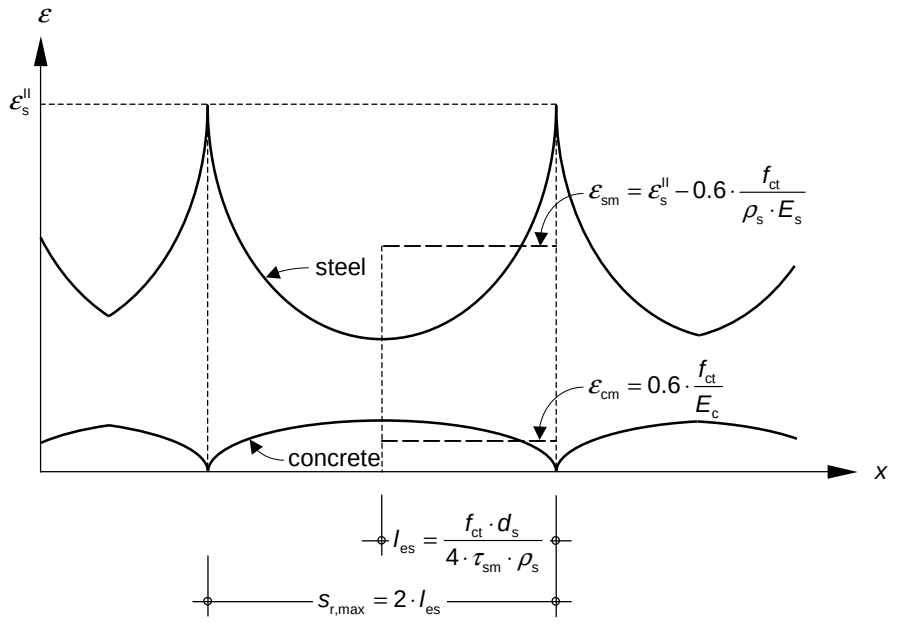

Fig. 2.5 Strains at stabilised cracking for the border case $s_{r,max} = 2 \cdot l_{es}$

Influence of Shrinkage

If the influence of shrinkage on the crack width shall be considered at stabilised cracking, this has at first no effect on the crack distribution or the possible crack spacings, as shown in section 2.1. However, according to fig. 2.6 an influence of the shrinkage on the development of concrete strain is evident. Because the concrete strain in the crack is, compared to the case without shrinkage, reduced by $\varepsilon^*_{s,shr}$ according to equation (2.12), the difference between the strains of steel and concrete is increased by the amount of $\varepsilon^*_{s,shr}$ compared to pure action of loading. It follows:

$$\varepsilon_{sm} = \varepsilon_s^{II} - 0.6 \cdot \frac{f_{ct}}{\rho_s \cdot E_s} \tag{2.25}$$

$$\varepsilon_{cm} = 0.6 \cdot \frac{f_{ct}}{\rho_s \cdot E_s} \cdot \alpha_E \cdot \rho_s + \varepsilon^*_{s,shr} \tag{2.26}$$

Considering the influence of shrinkage, the maximum crack width at stabilised cracking amounts to

$$w_{max} = s_{r,max} \cdot (\varepsilon_{sm} - \varepsilon_{cm}) = \frac{f_{ct} \cdot d_s}{2 \cdot E_s \cdot \tau_{sm} \cdot \rho_s} \cdot \left[\sigma_s - \left(0.6 \cdot \frac{f_{ct}}{\rho_s} + \varepsilon_{s,shr} \cdot E_s \right) \cdot (1 + \alpha_E \cdot \rho_s) \right] \tag{2.27}$$

Thus, the same external tensile load *F* leads to larger crack widths at the state of stabilised cracking when shrinkage is considered.

If the concrete strain caused by the action of loading is neglected, the required reinforcement to limit the crack width at stabilised cracking can be obtained directly by transforming the equations (2.24) and (2.27):

$$A_s = \sqrt{\frac{d_s \cdot F_{cr} \cdot (F_s - 0.6 \cdot F_{cr})}{2 \cdot w_k \cdot \tau_{sm} \cdot E_s}} \quad \text{(without influence of shrinkage)} \tag{2.28}$$

$$A_s = \Omega \cdot \left(-\varepsilon^*_{s,shr} + \sqrt{{\varepsilon^*_{s,shr}}^2 + \frac{2 \cdot (F_s - 0.6 \cdot F_{cr})}{\Omega \cdot E_s}} \right) \text{(considering influence of shrinkage)} \tag{2.29}$$

with $$\Omega = \frac{F_{cr} \cdot d_s}{4 \cdot w_k \cdot \tau_{sm}} \tag{2.30}$$

F_s tensile force, carried by the reinforcement in the crack

F_{cr} cracking force of the cross section

$$F_{cr} = A_c \cdot f_{ct} \tag{2.31}$$

$\varepsilon^*_{s,shr}$ concrete strain at crack surface after crack formation, considering shrinkage and relaxation of concrete; approximately equal to the free shrinkage coefficient of concrete

If the effective zone of the reinforcement does not cover the entire concrete tensile zone in the uncracked state, then for the calculation of crack width and crack spacing at stabilised cracking the cross section area A_c has to be replaced by the effective area of concrete in tension $A_{c,eff}$ (effective zone of the reinforcement).

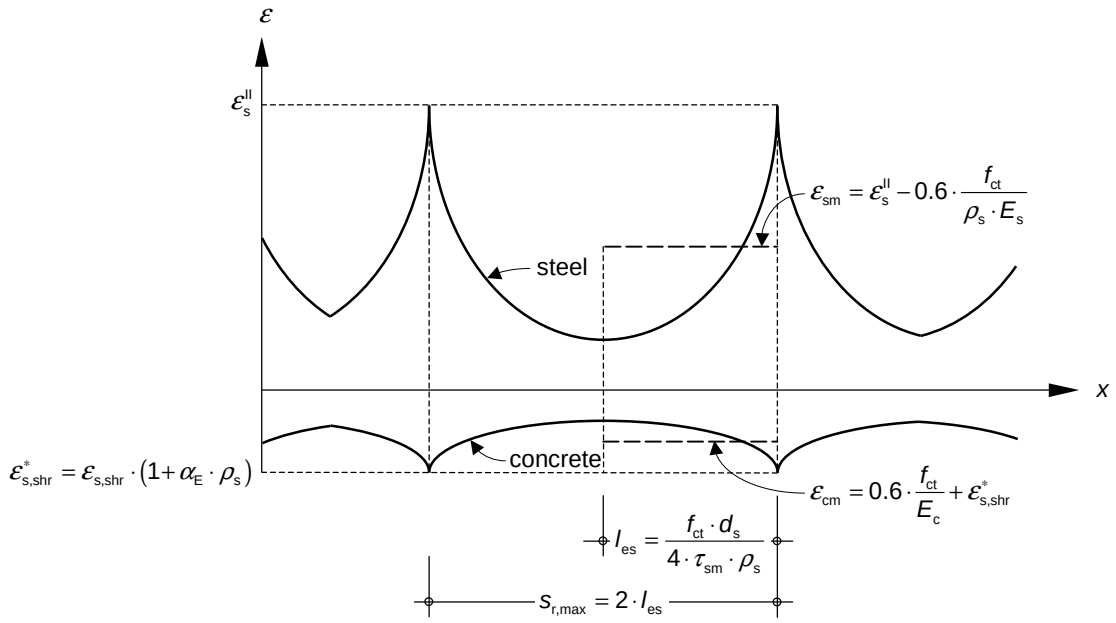

Fig. 2.6 Strains of steel and concrete at stabilised cracking for the border case $s_{r,max} = 2 \cdot l_{es}$ considering the influence of shrinkage

3 Stress-Crack Opening-Relationship of Fibre Concrete under Short Term Loading

Modelling the stress-crack opening-behaviour, the tensile strength of the plain concrete matrix f_{ct}, the cracking stress of the transformed cross section $\sigma_{cf,cr}$, the imaginary cracking stress of the fibre-reinforced concrete $\sigma^i_{cf,cr}$, as well as the fibre efficiency σ_{cf0} (maximum tensile stress of the cracked fibre-reinforced concrete) have to be discerned (fig. 3.1).

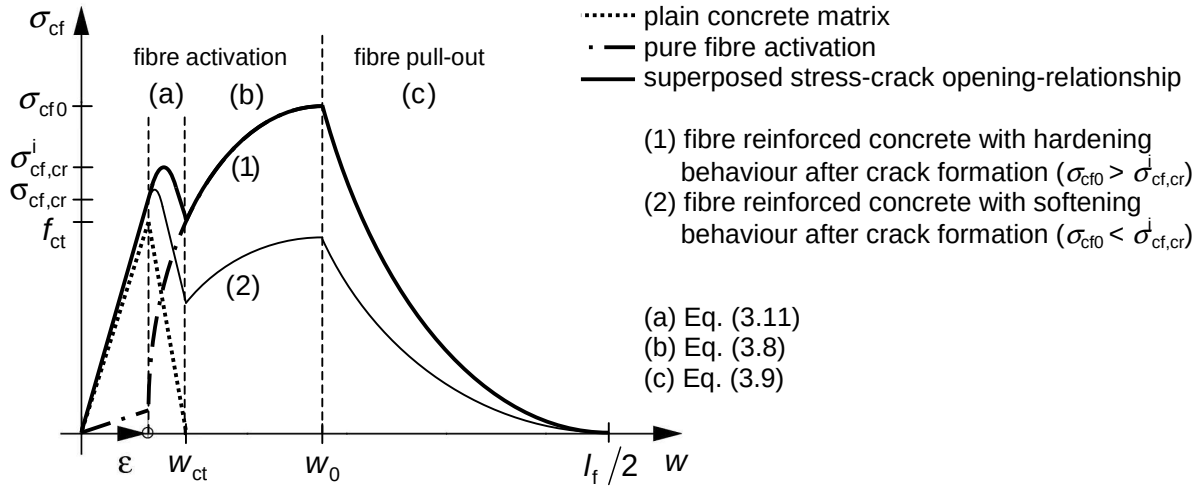

Fig. 3.1 Stress-crack opening-relationship of fibre-reinforced concrete, acc. to *Leutbecher* [DAfStb08]

Until reaching the cracking stress $\sigma_{cf,cr}$ of the transformed cross section, the fibre-reinforced concrete behaves widely linear-elastic (uncracked state). The fibres participate in the load transfer according to their tension stiffness referred to the total stiffness of the tensile specimen.

According to *Reinhardt* [Rei05], the cracking force of the fibre-reinforced concrete compared to the unreinforced matrix increases by the factor

$$\gamma = 1 + \rho_f \cdot (\eta \cdot \alpha_E - 1) \tag{3.1}$$

with ρ_f fibre content
η coefficient of fibre orientation
α_E relationship between the moduli of elasticity of fibres and concrete matrix

Equation (3.1) considers that, although the entire fibre volume displaces concrete matrix, in contrast to reinforced concrete only the proportion of fibres described by the fibre orientation coefficient is effective in tensile direction. For small fibre contents and because of the lower workability of the fresh concrete caused by the fibres, which entails frequently a higher air void content of the fibre-reinforced concrete and thus a smaller matrix strength, the cracking stress $\sigma_{cf,cr}$ of the transformed cross section actually increases hardly compared to the matrix strength.

With incipient cracking, the forces that have to be transferred between the crack surfaces are carried jointly at small crack widths by the matrix which softens in the opening crack and by the already activated fibres. A stable growth of microcracks starts. The imaginary cracking stress of the fibre-reinforced concrete $\sigma^{i}_{cf,cr}$ marks as a (local) maximum the transition to the macro crack. Contrary to the cracking stress $\sigma_{cf,cr}$ of the transformed cross section, the imaginary cracking stress of the fibre-reinforced concrete $\sigma^{i}_{cf,cr}$ increases significantly with the fibre content.

The fibre efficiency σ_{cf0} represents the maximum load-carrying capacity of the fibres in the cracked state. For short fibres, for which rupture before the complete activation is avoided, it marks at the same time the transition from the phase of fibre activation to the phase of fibre pull-out. Depending on the type of fibre and the fibre content, the fibre efficiency can be smaller or larger than the imaginary cracking stress of the fibre-reinforced concrete. Accordingly, the fibre-reinforced concrete shows a pure softening behaviour after cracking or a hardening behaviour with pronounced multiple cracking. In the case that the fibres are exclusively oriented parallel to the tension direction, the fibre efficiency σ_{cf0} can be derived due to theoretical considerations ([Li92, Beh96, Pfy03, Jun06, Leu07] amongst others):

$$\sigma_{cf0} = \rho_f \cdot \frac{\tau_{fm} \cdot l_f}{d_f} \qquad \text{(fibres exclusively oriented in tensile direction)} \tag{3.2}$$

with τ_{fm} average bond stress between fibre and matrix
l_f length of fibre
d_f diameter of fibre

Thereby, the average bond stress τ_{fm} can be appreciated for UHPC-matrixes and smooth steel wire fibres as follows:

$$\tau_{fm} = 1.3 \cdot f_{ctm} \tag{3.3}$$

with f_{ctm} mean centric tensile strength of the plain concrete matrix

The fibre efficiency according to equation (3.2) is reached computationally at a crack width w_0 according to equation (3.6).

$$w_0 = \frac{\tau_{fm} \cdot l_f^2}{E_f \cdot d_f} \tag{3.6}$$

with E_f modulus of elasticity of the fibre material

To consider the influence of fibre orientations deviating from tensile direction, equation (3.2) can be extended as follows:

$$\sigma_{cf0} = \eta \cdot g \cdot \rho_f \cdot \frac{\tau_{fm} \cdot l_f}{d_f} \qquad \text{(fibres with arbitrary orientation)} \tag{3.7}$$

with η coefficient of fibre orientation
g coefficient of fibre efficiency

The coefficient of fibre efficiency g in equation (3.7) considers the different pull-out resistance of the fibres oriented with different angles of inclination and the degradation of bond conditions by matrix flakings near the emersion point of the fibre as well as by the interaction of the fibres pulled-out within a group of fibres. Therefore, the coefficient of fibre efficiency is also called damage factor.

The fibre efficiency can be determined in centric tensile tests on notched specimens. Fibres that do not cross the crack orthogonally have to be straightened firstly when they are activated (fig. 3.2). Therefore, depending on the fibre orientation, σ_{cf0} is usually reached within a test at a somewhat larger crack width than predicted by equation (3.6).

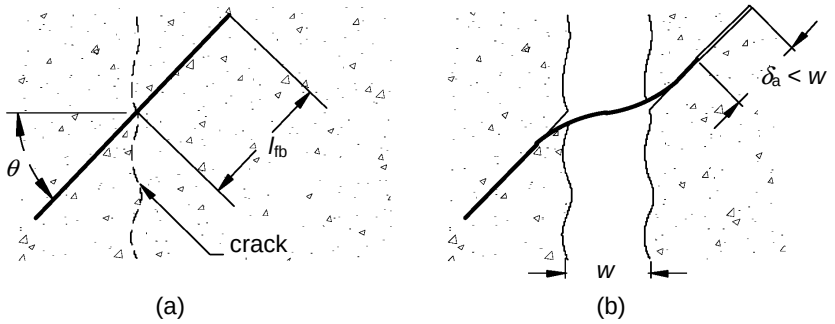

Fig. 3.2 Deflection of a fibre inclined to the crack direction [Voo03]
a) Fibre crossing a crack
b) Fibre pull-out

The tensile stress of the fibre-reinforced concrete transferred over a macro crack can be described according to equation (3.8) in the fibre activation phase and according to equation (3.9) in the fibre pull-out phase:

$$\sigma_{cf} = \sigma_{cf0} \cdot \left(2 \cdot \sqrt{\frac{w}{w_0}} - \frac{w}{w_0} \right) \qquad \text{(phase of fibre activation)} \tag{3.8}$$

$$\sigma_{cf} = \sigma_{cf0} \cdot \left(1 - 2 \cdot \frac{w}{l_f} \right)^2 \qquad \text{(phase of fibre pull-out)} \tag{3.9}$$

with σ_{cf0} fibre efficiency according to equation (3.7)
w actual crack width
w_0 crack width according to equation (3.6), referred to the fibre efficiency

Equation (3.9) provides a good agreement with test results especially for short fibres. If matrix flaking at the emersion point of the fibre (e.g. due to high defection forces for long fibres) or fibre rupture play a substantial role, then also a more rapid softening than predicted by equation (3.9) can be observed in the phase of fibre pull-out. Compared to the rise of tensile stress in the activation phase, the stress transferred by the fibres in the pull-out phase decreases however only slowly with increasing crack width. Therefore, in the margin of deformations relevant for the limitation of crack width in good approximation also a constant course on the level of the fibre efficiency can be accepted instead of equation (3.9).

$$\sigma_{cf} = \sigma_{cf0} \qquad \text{(phase of fibre pull-out, simplification for crack width control)} \qquad (3.10)$$

Within the range of very small crack widths, the stress-crack opening-relationship of the fibre-reinforced concrete is received by superposition of the descending branch of the matrix (fictitious crack model according to *Hillerborg* [Hil76]) and the equation (3.8) for the fibre activation. If the cracking stress of the transformed cross section $\sigma_{cf,cr}$ is approximately equal to the matrix tensile strength, the stress-crack opening-relationship results in

$$\sigma_{cf} = f_{ct} \cdot \left(1 - \frac{w \cdot f_{ct}}{2 \cdot G_F}\right) + \sigma_{cf0} \cdot \left(2 \cdot \sqrt{\frac{w}{w_0}} - \frac{w}{w_0}\right) \qquad (3.11)$$

with G_F fracture energy of the plain concrete matrix

Equation (3.11) is based on a linear descending branch of the stress-crack opening-relationship representing the matrix (fig. 3.3a), as it is recommended in [Ma03] for fine-aggregate UHPC (maximum aggregate size 0.5 up to 1 mm). The fracture energy can be assumed independently from the compressive strength to be approximately 50 up to 60 N/m. If a bi-linear softening branch is adequate (e.g. for normal-strength concrete or coarse-aggregate UHPC), in the aforementioned relationships only the part of the fracture energy marked in grey colour in fig. 3.3b may be considered as G_F (the initial descending is proper).

The crack width w^* for which equation (3.11) becomes maximum, can be found setting the first derivation to zero. One obtains

$$w^* = \frac{w_0}{\left(1 + \frac{w_0 \cdot f_{ct}^2 \cdot g}{2 \cdot \sigma_{cf0} \cdot G_F}\right)^2} \qquad (3.12)$$

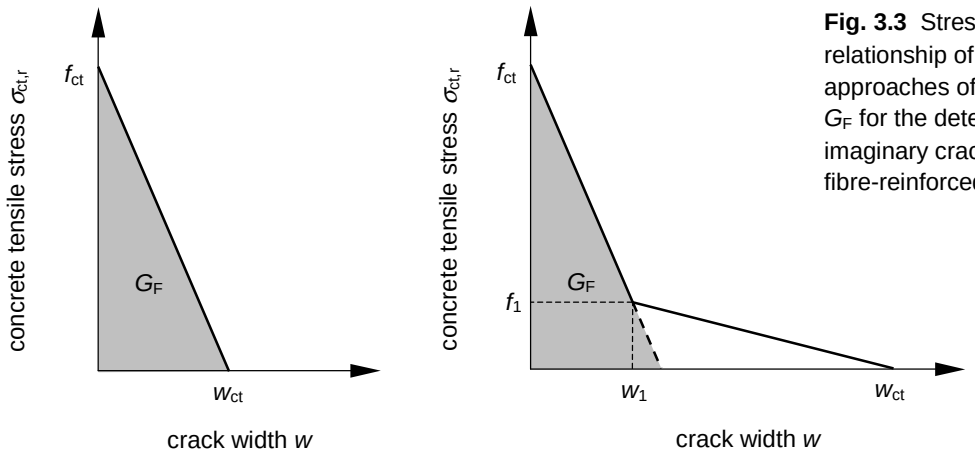

Fig. 3.3 Stress-crack opening-relationship of the matrix and approaches of the fracture energy G_F for the determination of the imaginary cracking stress of the fibre-reinforced concrete $\sigma^i_{cf,cr}$

The coefficient of fibre efficiency *g* in equation (3.12) is determined as follows from the fibre efficiency received in centric tensile tests:

$$g = \frac{\sigma_{cf0} \cdot d_f}{\eta \cdot \rho_f \cdot \tau_{fm} \cdot l_f} \tag{3.13}$$

The coefficient of fibre orientation η can be determined either experimentally or computationally in an appropriate way (e.g. according to the approach of [AFGC02]). Thereby, as both the investigations of *Markovic* [Mar06] and the revision of the tests of *Leutbecher* [Leu07] show, a predominantly two-dimensional fibre orientation orthogonally to the casting direction can be assumed in good approximation for fibres with a slenderness $\lambda_f \geq 80$. However, for compact fibres the orientation is widely three-dimensional.

If there exist doubts regarding the fibre orientation, on the safe side an predominantly two-dimensional fibre orientation should be chosen when evaluating equation (3.13). In this way, the coefficient of fibre efficiency *g* is likely to be overestimated and the imaginary cracking stress of the fibre-reinforced concrete is likely to be underestimated.

The imaginary cracking stress of the fibre-reinforced concrete $\sigma^{i}_{cf,cr}$ amounts approximately to

$$\sigma^{i}_{cf,cr} = f_{ct} \cdot \left(1 - \frac{w^* \cdot f_{ct}}{2 \cdot G_F}\right) + \sigma_{cf0} \cdot \left(2 \cdot \sqrt{\frac{w^*}{w_0}} - \frac{w^*}{w_0}\right) \tag{3.14}$$

with w^* crack width according to equation (3.12), referred to $\sigma^{i}_{cf,cr}$

The stress-crack opening-relationship represented qualitatively in fig. 3.1 has been confirmed experimentally in centric tensile tests on UHPC reinforced with different fibres and fibre contents [Leu07]. Besides, in [Leu07] the equations (3.8) and (3.9) have been extended to enable the consideration of the influence of shrinking on the stress-crack opening-relationship.

4 Limitation of Crack Width under Short Term Loading for Combined Reinforcement of Rebars and Fibres

4.1 Crack Width of a Single Crack

If the external load is increased beyond the imaginary cracking stress of a tensile member reinforced with rebars and fibres, firstly a softening behaviour results from the superposition of the concrete softening and the stress increase in the reinforcement. For the fibre-reinforced concrete this is represented in principle in fig. 3.1. Under force controlled loading thus an unstable crack growth of one of the microcracks results within the fracture process zones, until the fibre and the bar reinforcement are sufficiently activated in order to transfer the external tensile load in the macro crack without contribution of the concrete. Considering equilibrium of forces in the crack leads to:

$$F_{cr} = A_c \cdot \left(1 + \alpha_E \cdot \rho_s\right) \cdot \sigma^{i}_{cf,cr} = F_s + F_f = \sigma_s \cdot A_s + \sigma_{cf} \cdot A_c \tag{4.1}$$

with F_{cr} cracking force of the tensile member
F_s tensile force, carried by the bar reinforcement in the crack
F_f tensile force, carried by the fibres in the crack

In contrast to equation (2.1), the matrix tensile strength is replaced by the imaginary cracking stress of the fibre-reinforced concrete $\sigma^{i}_{cf,cr}$.

Assuming that the cross sections remain plane, the distribution of the total tensile force to the two types of reinforcement has to consider that the relative displacement between rebars and concrete matrix on the one hand as well as between the fibre reinforcement and the concrete matrix on the other hand must lead to same crack width (compatibility).

Due to the contribution of the fibres to the transfer of the tensile force in the crack, the tensile stress of the bar reinforcement in a single crack decreases to

$$\sigma_s = \frac{\left(1+\alpha_E \cdot \rho_s\right) \cdot \sigma_{cf,cr}^{i} - \sigma_{cf}}{\rho_s} \tag{4.2}$$

Through this, the load transmission length l_{es} of the bar reinforcement is reduced to

$$l_{es} = \frac{\left(\sigma_s - \sigma_{cf,cr}^{i} \cdot \alpha_E\right) \cdot d_s}{4 \cdot \tau_{sm}} = \frac{\left(\sigma_{cf,cr}^{i} - \sigma_{cf}\right) \cdot d_s}{4 \cdot \tau_{sm} \cdot \rho_s} \tag{4.3}$$

Thereby, the steel and concrete strains averaged over the load transmission lengths, ε_{sm} and ε_{cm}, can be determined analogously again according to equations (2.5) and (2.6). Fig. 4.1 shows qualitatively the courses of strain of the bar reinforcement, of the concrete matrix, and of a fibre, crossing the crack centrically. The index „I-II“ represents the state of micro-cracking, i.e. the transition from the uncracked state to the completely cracked state (macro crack), and marks the strain referred to the imaginary cracking stress of the fibre-reinforced concrete $\sigma_{cf,cr}^{i}$.

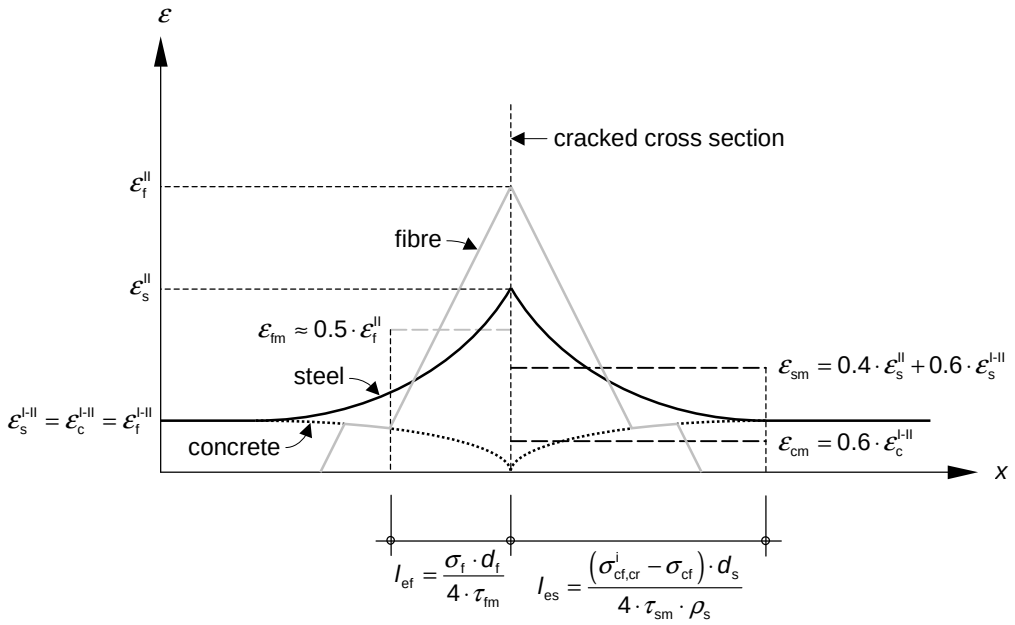

Fig. 4.1 Qualitative courses of strain of the bar reinforcement, of a fibre, crossing the crack centrically, and of the concrete matrix for a single crack

The width of a single crack *w* of a tensile member reinforced with rebars and fibres amounts to

$$\begin{aligned} w &= 2 \cdot l_{es} \cdot \left(\varepsilon_{sm} - \varepsilon_{cm}\right) \\ &= \frac{\left(\sigma_s - \sigma_{cf,cr}^{i} \cdot \alpha_E\right) \cdot d_s}{5 \cdot E_s \cdot \tau_{sm}} \cdot \sigma_s = \frac{\left(\sigma_{cf,cr}^{i} - \sigma_{cf}\right) \cdot d_s}{5 \cdot E_s \cdot \tau_{sm} \cdot \rho_s^2} \cdot \left[\left(1+\alpha_E \cdot \rho_s\right) \cdot \sigma_{cf,cr}^{i} - \sigma_{cf}\right] \end{aligned} \tag{4.4}$$

Because the tensile stress of fibre-reinforced concrete σ_{cf} depends itself on the crack width, the crack width according to equation (4.4) can be determined only iteratively. In contrast, if the limit of the crack width is known, then the required bar reinforcement can be calculated directly neglecting the average concrete strain caused by the action of loading:

$$A_s = \sqrt{\frac{\left(F - F_f\right)^2 \cdot d_s}{5 \cdot E_s \cdot \tau_{sm} \cdot w_k}} \qquad \text{(without influence of shrinkage)} \qquad (4.5)$$

$$A_s = \frac{F - F_f}{\sqrt{\frac{5 \cdot E_s \cdot \tau_{sm} \cdot w_k}{d_s}} + \varepsilon^*_{shr} \cdot E_s} \qquad \text{(considering influence of shrinkage)} \qquad (4.6)$$

with F total external tensile load in the crack

F_f tensile load, carried by the fibres in the crack

$$F_f = A_c \cdot \sigma_{cf} \qquad (4.7)$$

ε^*_{shr} concrete strain at crack surface after crack formation, considering shrinkage and relaxation of concrete; approximately equal to the free shrinkage coefficient of concrete

If *n* different types of fibre (fibre cocktail) are combined with one kind of bar reinforcement, then in equations (4.5) and (4.6) the tensile stress of fibre-reinforced concrete σ_{cf} is to be determined from the sum of the contributions of the *n* types of fibre.

With the cracking force of the concrete cross section (action of restraint), the required bar reinforcement arises independently of the size of the shrinkage coefficient:

$$A_s = A_c \cdot \left(\sigma^i_{cf,cr} - \sigma_{cf}\right) \cdot \sqrt{\frac{d_s}{5 \cdot E_s \cdot \tau_{sm} \cdot w_k}} \qquad (4.8)$$

4.2 Stabilised Cracking and Progressive Crack Formation

Similar to a reinforced concrete tensile member also cross sections with higher imaginary cracking stress $\sigma^i_{cf,cr}$, which are outside of the load transmission lengths of already existing cracks, crack under further load increase, until a difference between the strains of concrete matrix and bar reinforcement exists everywhere (state of stabilised cracking). The spacing of these cracks amounts then, similar to the stabilised cracking of a reinforced concrete tensile member, to the simple ($s_{r,min}$) up to the double load transmission length ($s_{r,max}$) of the bar reinforcement according to equation (4.3).

In fig. 4.2, the courses of strain in the state of stabilised cracking are depicted qualitatively for the case that shrinkage is neglected.

In the state of stabilised cracking a new crack arises if between the end of the transmission length of the fibres and that of the bar reinforcement the imaginary cracking stress of the fibre-reinforced concrete $\sigma^i_{cf,cr}$ is reached again (progressive crack formation). This can be achieved due to the increase of the bond stress between concrete and bar reinforcement according to the bond stress-slip-relationship as well as by further fibre activation. The latter requires, that the fibres are not yet in the pull-out phase after single cracking. With the fibre contents and fibre dimensions common for UHPC, this condition is generally met. As confirmed by the investigations in [Leu07], the fibre-reinforced concrete itself does not have to show a hardening behaviour.

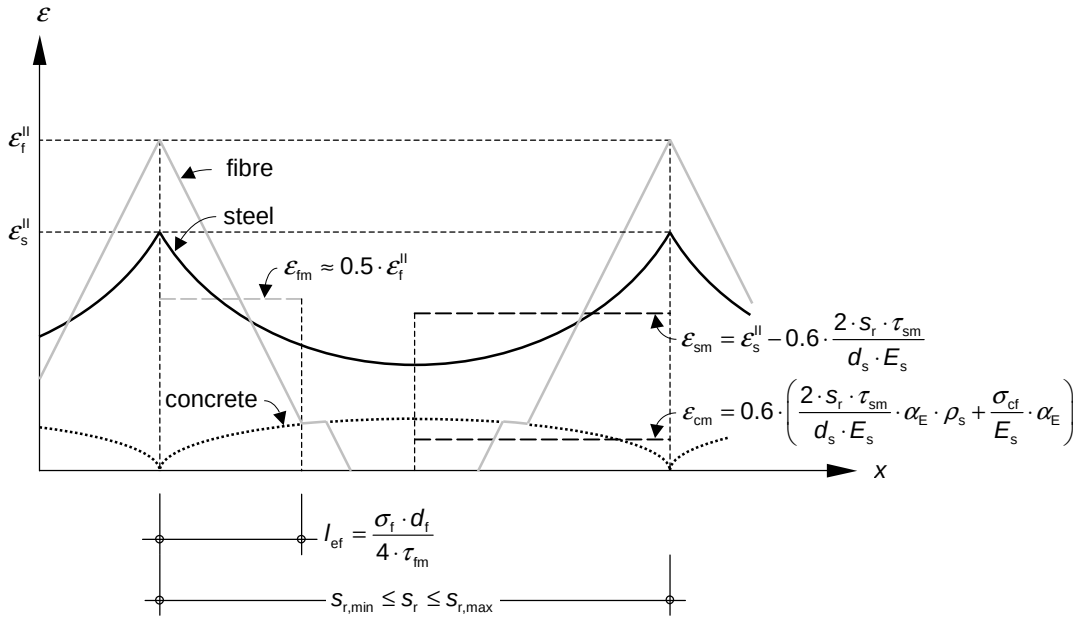

Fig. 4.2 Qualitative courses of strain of the bar reinforcement, of a fibre, crossing the crack centrically, and of the concrete matrix in the state of stabilised cracking

Assuming a constant matrix tensile strength and an even fibre distribution, the following condition for the formation of a new crack can be derived:

$$\frac{2 \cdot s_r \cdot \tau_{sm}}{d_s} \cdot \rho_s + \sigma_{cf}(w) \ge \sigma_{cf,cr}^{i} \tag{4.9}$$

The first term in equation (4.9) represents the concrete tensile stress introduced from the bar reinforcement into the concrete by bond action. The second expression corresponds with the load contribution of the fibres in the crack according to equation (3.8) or (3.10).

Depending on the different bond behaviour of the bar reinforcement and the fibres, the crack spacings halve themselves under further load increase continuously, until either the fibres get into the pull-out phase after complete activation (case A, fig. 4.3a) or, for fibre concretes with hardening behaviour, the crack spacings become so small that also the load transmission length of the fibres affect each other at adjacent cracks before the fibre efficiency is reached ($s_r \le 2 \cdot l_{ef}$, case B, fig. 4.3b). The latter means, that in the centre between two existing cracks, not the entire tensile load carried by the fibres in the crack is available, in order to form a new crack. For both cases the mechanical relationships are deduced in [Leu07].

In the following, exclusively the case with short fibres and low fibre contents, in which fibre pull-out is proper for the end of progressive crack formation (case A), is contemplated.

Transformation of equation (4.9) delivers for this case the following maximum crack spacing in the phase of progressive crack formation:

$$s_{r,max} = \frac{\left(\sigma_{cf,cr}^{i} - \sigma_{cf}\right) \cdot d_s}{2 \cdot \tau_{sm} \cdot \rho_s} \tag{4.10}$$

The steel strain averaged over the maximum crack spacing amounts to

$$\varepsilon_{sm} = \varepsilon_s^{II} - 0.6 \cdot \frac{\left(\sigma_{cf,cr}^{i} - \sigma_{cf}\right)}{E_s \cdot \rho_s} \tag{4.11}$$

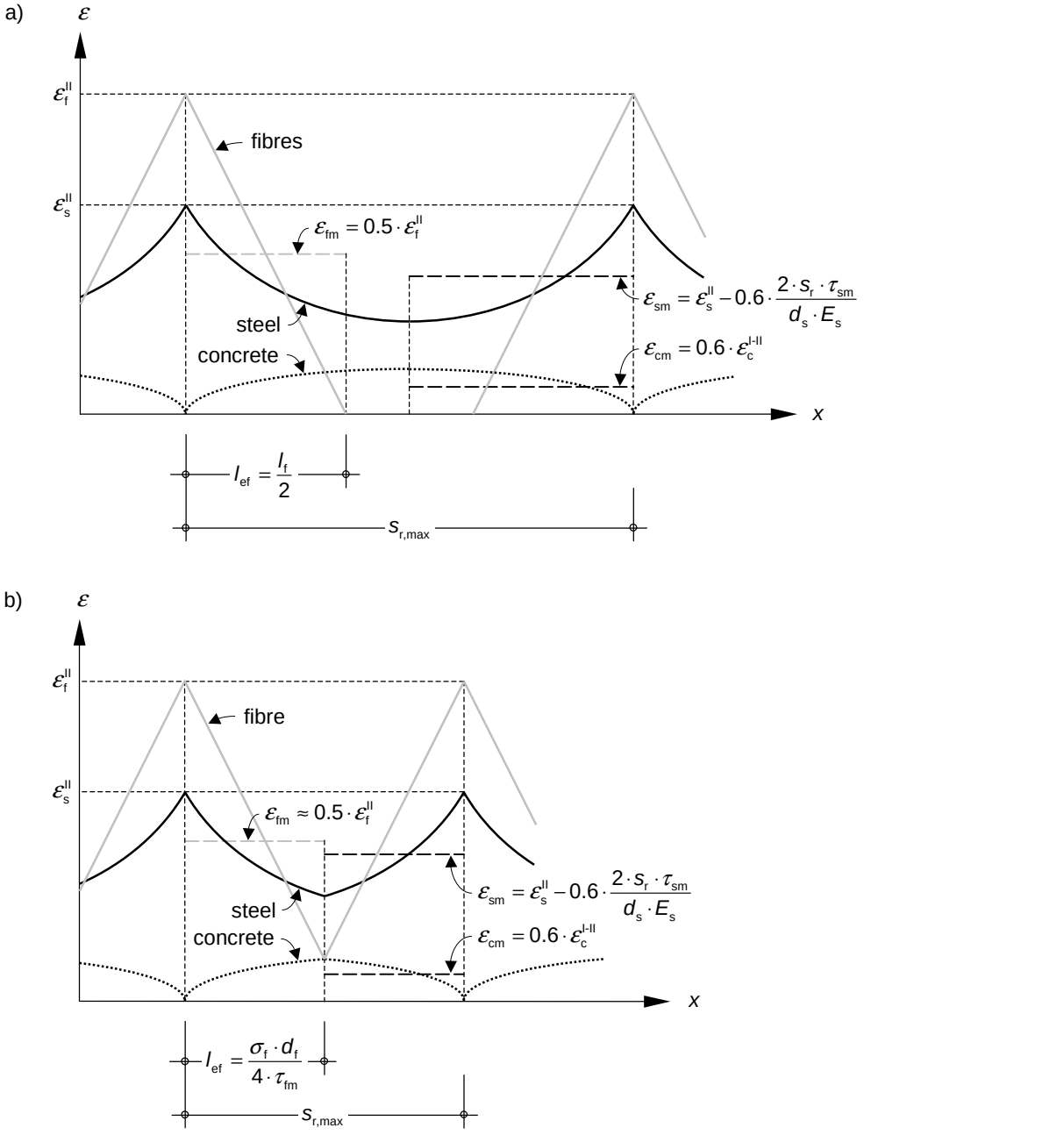

Fig. 4.3 Qualitative courses of strain of the bar reinforcement, of a fibre, crossing the crack centrically, and of the concrete matrix in the phase of progressive crack formation
a) Case A: Transition to the fibre pull-out phase
a) Case B: Load transmission lengths of the fibres influence themselves mutually ($s_r \le 2\ l_{ef}$; further details see [Leu07])

The average concrete strain is

$$\varepsilon_{cm} = 0.6 \cdot \frac{\sigma^{i}_{cf,cr}}{E_s \cdot \rho_s} \cdot \alpha_E \cdot \rho_s \tag{4.12}$$

The maximum crack width can then be calculated as follows:

$$\begin{aligned} w_{max} &= s_{r,max} \cdot \left(\varepsilon_{sm} - \varepsilon_{cm}\right) \\ &= \frac{\left(\sigma^{i}_{cf,cr} - \sigma_{cf}\right) \cdot d_s}{2 \cdot E_s \cdot \tau_{sm} \cdot \rho_s} \cdot \left[\sigma_s - 0.6 \cdot \frac{\sigma^{i}_{cf,cr}}{\rho_s} \cdot \left(1 + \alpha_E \cdot \rho_s\right) + 0.6 \cdot \frac{\sigma_{cf}}{\rho_s}\right] \end{aligned} \tag{4.13}$$

In equation (4.13) the steel stress in the crack is

$$\sigma_s = \frac{F}{A_s} - \frac{\sigma_{cf}}{\rho_s} \tag{4.14}$$

After complete activation of the fibres (reaching the fibre efficiency), a new crack can only be initiated by an increase of the bond stress between concrete and bar reinforcement. If rigid-plastic bond law is assumed for the bar reinforcement, the crack pattern is completed when reaching the fibre efficiency.

Neglecting the average concrete strain, the required bar reinforcement in the phase of progressive crack formation can be determined directly transforming the equation (4.13) as follows:

$$A_s = \sqrt{\frac{\left[\left(F - F_f\right) - 0.6 \cdot \left(F_{f,cr} - F_f\right)\right] \cdot \left(F_{f,cr} - F_f\right) \cdot d_s}{2 \cdot E_s \cdot \tau_{sm} \cdot w_k}} \qquad \text{(without shrinkage)} \tag{4.15}$$

with F total external tensile load

F_f tensile load, carried by the fibres in the crack

$$F_f = A_c \cdot \sigma_{cf} \tag{4.7}$$

$F_{f,cr}$ cracking force of the cross section of the fibre-reinforced concrete

$$F_{f,cr} = A_c \cdot \sigma_{cf,cr}^{i} \tag{4.16}$$

Considering the influence of shrinkage results in

$$A_s = \Omega \cdot \left(-\varepsilon_{shr}^{*} + \sqrt{\varepsilon_{shr}^{*\,2} + 2 \cdot \frac{\left(F - F_f\right) - 0.6 \cdot \left(F_{f,cr} - F_f\right)}{\Omega \cdot E_s}} \right) \quad \text{(considering shrinkage)} \tag{4.17}$$

with $$\Omega = \frac{\left(F_{f,cr} - F_f\right) \cdot d_s}{4 \cdot w_k \cdot \tau_{sm}} \tag{4.18}$$

F total external tensile load

F_f tensile load, carried by the fibres in the crack

$$F_f = A_c \cdot \sigma_{cf} \tag{4.7}$$

$F_{f,cr}$ cracking force of the cross section of the fibre-reinforced concrete

$$F_{f,cr} = A_c \cdot \sigma_{cf,cr}^{i} \tag{4.16}$$

ε_{shr}^{*} concrete strain at the crack surface after cracking considering the influences of shrinkage und relaxation of concrete; approximately equal to the free shrinkage coefficient of the concrete

For the cracking force of the cross section F_{cr} (tensile stresses caused by the action of restraint), the required reinforcement A_s is independently of the size of the shrinkage coefficient and can therefore always be determined according to equation (4.15).

If the effective zone of the reinforcement does not cover the entire concrete tensile zone in the uncracked state, then for the calculation according to this section the cross section area A_c again has to be replaced by the effective area of concrete in tension $A_{c,eff}$. To what extent a fibre addition affects the sphere of action of the reinforcement has not been investigated so far.

5 Examples of Typical Applications

The application of the relationships derived in the previous sections to UHPC is illustrated in the following on the basis of two examples. The effects of long term and cyclic loading on the bond behaviour is thereby considered according to DIN 1045-1 [DIN01] by a reduction of the solidity coefficients from 0.6 down to 0.4 describing the course of the average concrete and steel strains. The transferability of this reduction valid for normal- and high-strength concretes to UHPC requires however still an experimental verification. In particular, the influence of long term and cyclic loading on the pull-out behaviour of the fibres is to be clarified.

5.1 Example 1: Limitation of Crack Width of a thin UHPC-Topping Layer for the Action of Restraint

Fig. 5.1 shows the cross section of a thin UHPC-topping layer, which is applied on an existing concrete slab for rehabilitation purposes. For the UHPC-topping layer the crack width is to be limited to $w_k = 0.05\,\text{mm}$ under centric restraint due to shrinkage. The bond between the UHPC-layer and the subfront is not subject of the present example.

Two cases are examined:

Z1: the restraint acts only in one direction (theoretical case); the UHPC-topping layer is reinforced uniaxially with rebars BSt 500 (Fig. 5.1a)

Z2: the UHPC-topping layer is reinforced orthogonally with rebars BSt 500 (Fig. 5.1b)

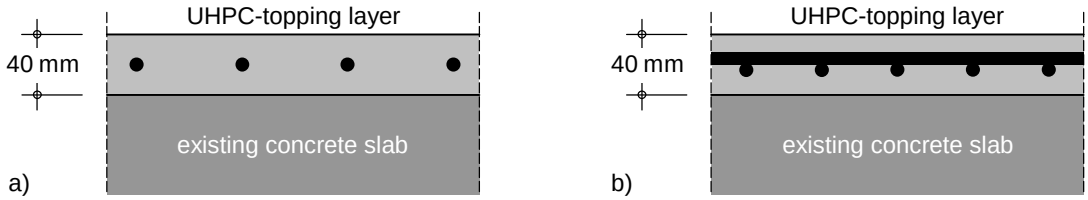

Fig. 5.1 Cross section of a thin UHPC-topping layer, applied on an existing concrete slab
a) reinforced uniaxially
b) reinforced orthogonally

The topping layer is made of a fine-aggregate UHPC of the mixture M2Q [Feh05]. 17 mm long steel wire fibres with a diameter of 0.15 mm are added. A rather small fibre content of $\rho_f = 0.9$ vol.-% shall be used in order to obtain an ecological and economic solution. For this fibre-reinforced concrete mixture the relevant strength parameters and other characteristics were determined directly by tests or analytically [Leu07]. The required parameters are summarised in table 5.1.

Table 5.1 Characteristics of the fibre-reinforced UHPC mixture

	UHPC-matrix		
1	- matrix tensile strength f_{ct}	in N/mm²	8.5
2	- fracture energy of the matrix G_F	in N/m	60
	fibres		
3	- fibre length l_f	in mm	17
4	- fibre diameter d_f	in mm	0.15
5	- modulus of elasticity E_f	in N/mm²	200,000
6	- fibre content ρ_f	in vol.-%	0.9
7	- bond stress τ_{fm}	in N/mm²	11
8	- coefficient of fibre efficiency g		1.13

Z1: UHPC-topping layer is reinforced uniaxially

According to the findings in [Leu07] concerning the fibre orientation, a predominantly two-dimensional fibre orientation perpendicularly to the casting direction is assumed. Because of absence of an influence of lateral formwork surfaces, the coefficient of fibre orientation amounts in the present case to

$$\eta = \eta_{2D} = 0.637$$

Thereby, the influence of the rebars on the fibre orientation has been neglected conservatively.

The average value of the fibre efficiency results according to equation (3.7) in:

$$\sigma_{cf0m} = \eta \cdot g \cdot \rho_f \cdot \frac{\tau_{fm} \cdot l_f}{d_f} = 0.637 \cdot 1.13 \cdot 0.009 \cdot \frac{11 \cdot 17}{0.15} = 8.08 \text{ N/mm}^2$$

Based on the results of investigations in [Leu07], the 5-% quantile of the fibre efficiency of the present fibre-reinforced concrete mix can be approximated as follows:

$$\sigma_{cf0k;0.05} = 0.7 \cdot \sigma_{cf0m} = 0.7 \cdot 8.08 = 5.66 \text{ N/mm}^2 \qquad \text{(5-\% quantile)}$$

The crack width referred to the fibre efficiency can be determined according to equation (3.6):

$$w_0 = \frac{\tau_{fm} \cdot l_f^2}{E_f \cdot d_f} = \frac{11 \cdot 17^2}{200{,}000 \cdot 0.15} = 0.106 \text{ mm}$$

The imaginary cracking stress of the fibre-reinforced concrete is calculated according to equations (3.12) and (3.14).

$$\sigma^{i}_{cf,cr\,k;0.05} = f_{ctm} \cdot \left(1 - \frac{w^* \cdot f_{ctm}}{2 \cdot G_F}\right) + \sigma_{cf0k;0.05} \cdot \left(2 \cdot \sqrt{\frac{w^*}{w_0}} - \frac{w^*}{w_0}\right)$$

$$= 8.5 \cdot \left(1 - \frac{0.56 \cdot 8.5}{2 \cdot 60}\right) + 5.66 \cdot \left(2 \cdot \sqrt{\frac{0.56 \cdot 10^{-3}}{0.106}} - \frac{0.56 \cdot 10^{-3}}{0.106}\right) = 8.96 \text{ N/mm}^2$$

using $\quad w^* = \dfrac{w_0}{\left(1 + \dfrac{w_0 \cdot f_{ctm}^2 \cdot g}{2 \cdot \sigma_{cf0k;0.05} \cdot G_F}\right)^2} = \dfrac{0.106 \cdot 10^3}{\left(1 + \dfrac{0.106 \cdot 8.5^2 \cdot 1.13}{2 \cdot 5.66 \cdot 60 \cdot 10^{-3}}\right)^2} = 0.56 \,\mu\text{m}$

According to equation (4.16), the cracking force of the fibre-reinforced cross section amounts to:

$$F_{f,cr} = A_c \cdot \sigma^{i}_{cf,cr\,k;0.05} = 0.040 \cdot 8.96 = 0.358 \text{ MN/m}$$

The tensile force carried by the fibres in the crack is determined according to equation (4.7):

$$F_f = A_c \cdot \sigma_{cf} = 0.040 \cdot 5.10 = 0.204 \text{ MN/m}$$

with $\quad \sigma_{cf} = \sigma_{cf0k;0.05} \cdot \left(2 \cdot \sqrt{\dfrac{w_k}{w_0}} - \dfrac{w_k}{w_0}\right) = 5.66 \cdot \left(2 \cdot \sqrt{\dfrac{0.05}{0.106}} - \dfrac{0.05}{0.106}\right) = 5.10 \text{ N/mm}^2$

Because the local imaginary cracking stress of the fibre-reinforced concrete $\sigma^{i}_{cf,cr}$ depends on the fibre distribution, the plateau in the stress-strain-relationship in the phase of single cracking, well known for reinforced concrete, can not be observed evidently. For pure action of loading this is without meaning. However, for restraint action as in the present case, the restraint depends significantly on the stiffness of the tensile member and thus on the crack formation. In order not to receive results on the unsafe side by underestimating the stiffness of a tensile member, the cracking stress of a cross section with favourable fibre efficiency (95 % quantile) should be assumed as restraint force.

The cracking stress is determined as before. However, $\sigma_{cf0k;0.05}$ is replaced by $\sigma_{cf0k;0.95}$. Assuming a symmetrical distribution of the fibre efficiency with respect to its mean value it results in:

$$\sigma_{cf0k;0.95} = 1.3 \cdot \sigma_{cf0m} = 1.3 \cdot 8.08 = 10.50 \text{ N/mm}^2 \qquad \text{(95-\% quantile)}$$

The upper quantile of the cracking force of the fibre-reinforced cross section amounts to

$$F_{f,cr;0.95} = A_c \cdot \sigma^{i}_{cf,cr\,k;0.95} = 0.040 \cdot 9.97 = 0.399 \text{ MN/m}$$

$$\text{with} \quad w^* = \frac{w_0}{\left(1 + \frac{w_0 \cdot f_{ctm}^2 \cdot g}{2 \cdot \sigma_{cf0k;0.95} \cdot G_F}\right)^2} = \frac{0.106 \cdot 10^3}{\left(1 + \frac{0.106 \cdot 8.5^2 \cdot 1.13}{2 \cdot 10.50 \cdot 60 \cdot 10^{-3}}\right)^2} = 1.71 \,\mu\text{m}$$

$$\sigma^{i}_{cf,cr\,k;0.95} = f_{ctm} \cdot \left(1 - \frac{w^* \cdot f_{ctm}}{2 \cdot G_F}\right) + \sigma_{cf0k;0.95} \cdot \left(2 \cdot \sqrt{\frac{w^*}{w_0}} - \frac{w^*}{w_0}\right)$$

$$= 8.5 \cdot \left(1 - \frac{1.71 \cdot 8.5}{2 \cdot 60}\right) + 10.50 \cdot \left(2 \cdot \sqrt{\frac{1.71 \cdot 10^{-3}}{0.106}} - \frac{1.71 \cdot 10^{-3}}{0.106}\right) = 9.97 \text{ N/mm}^2$$

Furthermore, the average bond stress τ_{sm} is needed in order to determine the required reinforcement for the limitation of crack width according to equation (4.15). If a linear relationship between the bond strength $\tau_{b\,max}$ and the mean matrix tensile strength f_{ctm} is assumed, then, based on pull-out tests on ribbed reinforcing bars with different relative rib areas, the normalised average bond stresses represented in fig. 5.2 are obtained (details see [Leu07]).

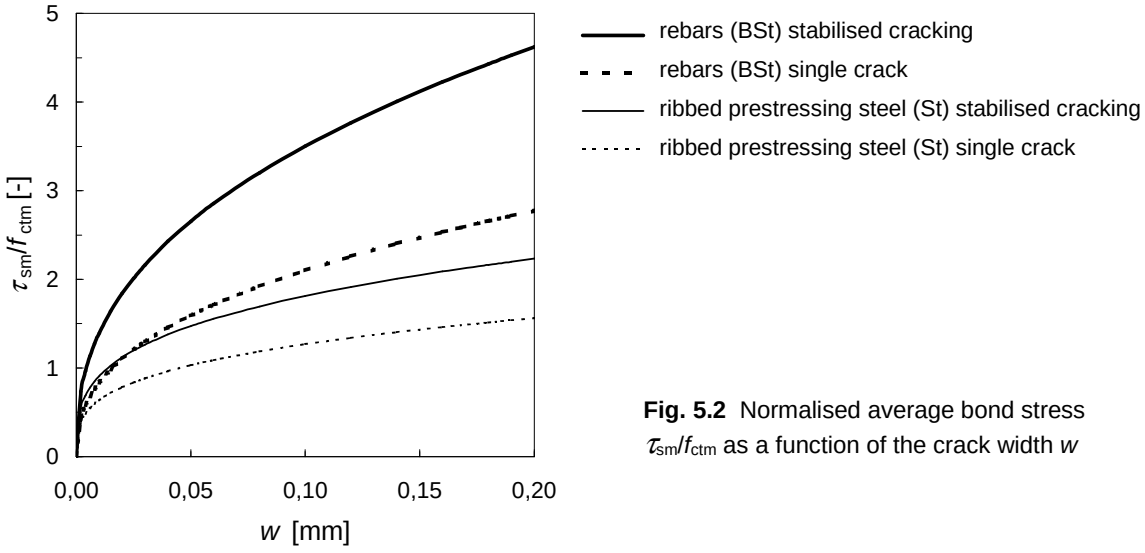

Fig. 5.2 Normalised average bond stress τ_{sm}/f_{ctm} as a function of the crack width w

For a crack width $w_k = 50\,\mu m$, demanded here and relevant especially regarding durability (effect of chlorides), the following values are obtained:

$$\tau_{sm} = 2.0 \cdot f_{ctm} \qquad \text{for rebars (BSt) with } f_R = 0.072 \qquad (5.1)$$

$$\tau_{sm} = 1.2 \cdot f_{ctm} \qquad \text{for ribbed prestressing steel (St) with } f_R = 0.024 \qquad (5.2)$$

For the present example, the evaluation of equations (5.1) and (5.2) results in

$$\tau_{sm} = 2.0 \cdot 8.5 = 17 \text{ N/mm}^2 \qquad \text{for rebars}$$

$$\tau_{sm} = 1.2 \cdot 8.5 = 10.2 \text{ N/mm}^2 \qquad \text{for ribbed prestressing steel}$$

If in equation (4.15) the degradation of the bond behaviour under long term loading is considered by a reduction of the solidity coefficient from 0.6 down to 0.4, as described before, then with $F = F_{f,cr;0.95}$, $\tau_{sm} = 17$ N/mm^2 (rebars BSt 500 S), and $d_s = 8$ mm the following is obtained:

$$A_s = \sqrt{\frac{\left[\left(F - F_f\right) - 0.4 \cdot \left(F_{f,cr} - F_f\right)\right] \cdot \left(F_{f,cr} - F_f\right) \cdot d_s}{2 \cdot w_k \cdot \tau_{sm} \cdot E_s}}$$

$$= 10^4 \cdot \sqrt{\frac{\left[\left(0.399 - 0.204\right) - 0.4 \cdot \left(0.358 - 0.204\right)\right] \cdot \left(0.358 - 0.204\right) \cdot 8}{2 \cdot 0.05 \cdot 17 \cdot 200{,}000}} = 6.95 \text{ cm}^2/\text{m}$$

According to equation (4.10), the maximum crack spacing results in

$$s_{r,max} = \frac{\left(F_{f,cr} - F_f\right) \cdot d_s}{2 \cdot \tau_{sm} \cdot A_s} = \frac{\left(0.358 - 0.204\right) \cdot 8}{2 \cdot 17 \cdot 6.95} \cdot 10^4 = 52 \text{ mm}$$

Z2: UHPC-topping layer is reinforced orthogonally

Compared to the topping layer reinforced uniaxially, the action of fibres is reduced significantly by the transverse reinforcing bars. Therefore, the load carried by the fibres is determined for a cross section diminished by a transverse reinforcing bar. However, the tensile force necessary to form a new crack is determined for an unweakened cross section. The further calculation corresponds to that of the previous example and is thus not described in the same detail as before.

The tensile force carried by the fibres in the crack in the region of a transverse reinforcing bar amounts to:

$$F_f = A_{c,red} \cdot \sigma_{cf} = \left(0.040 - 0.008\right) \cdot 5.10 = 0.163 \text{ MN/m}$$

If the degradation of the bond behaviour under long term loading is considered by a reduction of the solidity coefficient from 0.6 down to 0.4, the required reinforcement results in:

$$A_s = \sqrt{\frac{\left[\left(F - F_f\right) - 0.4 \cdot \left(F_{f,cr} - F_f\right)\right] \cdot \left(F_{f,cr} - F_f\right) \cdot d_s}{2 \cdot w_k \cdot \tau_{sm} \cdot E_s}}$$

$$= 10^4 \cdot \sqrt{\frac{\left[\left(0.399 - 0.163\right) - 0.4 \cdot \left(0.358 - 0.163\right)\right] \cdot \left(0.358 - 0.163\right) \cdot 8}{2 \cdot 0.05 \cdot 17 \cdot 200{,}000}} = 8.51 \text{ cm}^2/\text{m}$$

The maximum crack spacing is:

$$s_{r,max} = \frac{\left(F_{f,cr} - F_f\right) \cdot d_s}{2 \cdot \tau_{sm} \cdot A_s} = \frac{(0.358 - 0.163) \cdot 8}{2 \cdot 17 \cdot 8.51} \cdot 10^4 = 54 \text{ mm}$$

If the topping layer is reinforced orthogonally with an axial space of $a = 50$ mm ($d_s = 8$ mm/ $a = 50$ mm $\hat{=} 10.06$ cm^2/m), it is likely that a crack is formed near to every transverse reinforcing bar.

5.2 Example 2: Limitation of Crack Width of an UHPC Tensile Member under Action of Loading

Fig. 5.3 shows the cross and longitudinal section of an UHPC tensile member reinforced with four rebars, that has been heat treated after fabrication. The crack width is to be limited under serviceability load $F = 0.500$ MN to $w_k = 0.10$ mm.

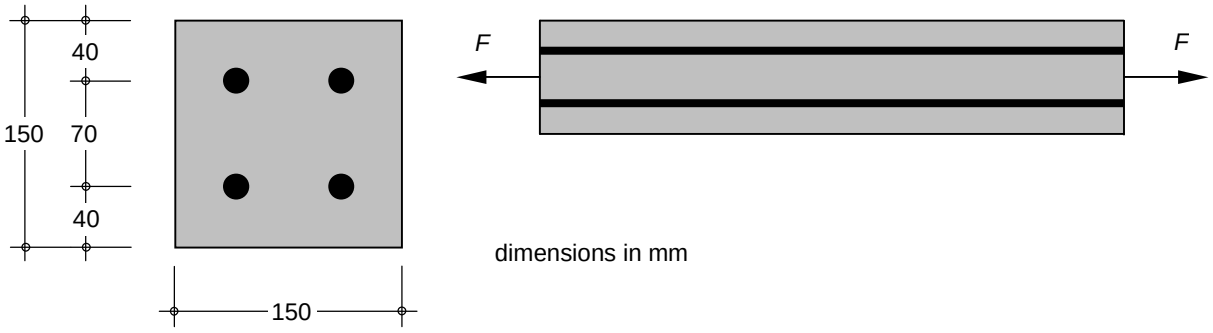

Fig. 5.3 Cross section (left hand side) and longitudinal section (right hand side) of an UHPC tensile member

Two cases are examined:

L1: the UHPC tensile member is reinforced with rebars and steel fibres

L2: the UHPC tensile member is reinforced only with rebars

Based on these two examples, the very favourable influence even of a small fibre content on the crack widths and on the required bar reinforcement shall be illustrated.

L1: The UHPC tensile member is reinforced with rebars and steel fibres

The same fibre-reinforced UHPC mixture as in example 1 is used. The required material and bond characteristics can be found in table 5.1.

Considering the favourable influence of the formwork surfaces according to fig. 5.4, the coefficient of fibre orientation results as follows, assuming a predominantly two-dimensional fibre orientation:

$$\eta = \frac{\eta_{1D} \cdot l_f + \eta_{2D} \cdot \left(b - l_f\right)}{b} = \frac{1.0 \cdot 17 + 0.637 \cdot (150 - 17)}{150} = 0.68$$

Thereby, the small influence of the reinforcing bars on the fibre orientation is neglected again.

The mean value of the fibre efficiency according to equation (3.7) amounts to:

$$\sigma_{\mathrm{cf0m}} = \eta \cdot g \cdot \rho_{\mathrm{f}} \cdot \frac{\tau_{\mathrm{fm}} \cdot l_{\mathrm{f}}}{d_{\mathrm{f}}} = 0.68 \cdot 1.13 \cdot 0.009 \cdot \frac{11 \cdot 17}{0.15} = 8.62 \text{ N/mm}^2$$

The characteristic value of the fibre efficiency is:

$$\sigma_{\mathrm{cf0k;0.05}} = 0.7 \cdot \sigma_{\mathrm{cf0m}} = 0.7 \cdot 8.62 = 6.03 \text{ N/mm}^2$$

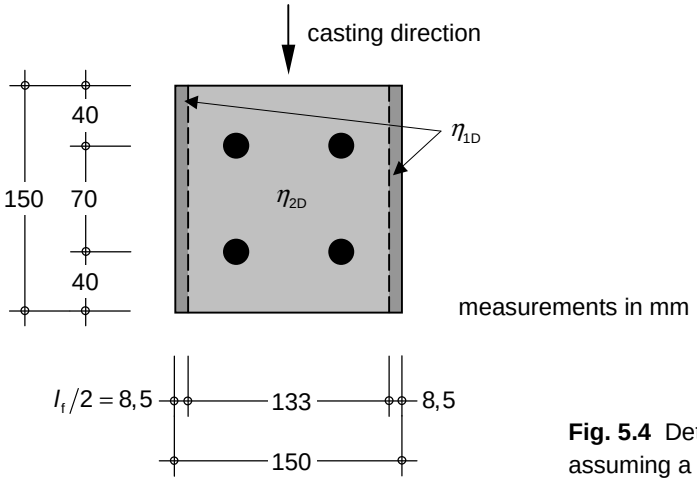

Fig. 5.4 Determination of the coefficient of fibre orientation assuming a predominantly two-dimensional fibre orientation

The imaginary cracking stress of fibre-reinforced concrete results according to equations (3.12) and (3.14) in:

$$\sigma^{\mathrm{i}}_{\mathrm{cf,cr\,k;0.05}} = f_{\mathrm{ctm}} \cdot \left(1 - \frac{w^* \cdot f_{\mathrm{ctm}}}{2 \cdot G_{\mathrm{F}}}\right) + \sigma_{\mathrm{cf0k;0.05}} \cdot \left(2 \cdot \sqrt{\frac{w^*}{w_0}} - \frac{w^*}{w_0}\right)$$

$$= 8.5 \cdot \left(1 - \frac{0.63 \cdot 8.5}{2 \cdot 60}\right) + 6.03 \cdot \left(2 \cdot \sqrt{\frac{0.63 \cdot 10^{-3}}{0.106}} - \frac{0.63 \cdot 10^{-3}}{0.106}\right) = 9.01 \text{ N/mm}^2$$

$$\text{using} \quad w^* = \frac{w_0}{\left(1 + \frac{w_0 \cdot f_{\mathrm{ctm}}^2 \cdot g}{2 \cdot \sigma_{\mathrm{cf0k;0.05}} \cdot G_{\mathrm{F}}}\right)^2} = \frac{0.106 \cdot 10^3}{\left(1 + \frac{0.106 \cdot 8.5^2 \cdot 1.13}{2 \cdot 6.03 \cdot 60 \cdot 10^{-3}}\right)^2} = 0.63 \,\mu\mathrm{m}$$

According to equation (4.16), the cracking force of the cross section of fibre-reinforced concrete amounts to

$$F_{\mathrm{f,cr}} = A_{\mathrm{c}} \cdot \sigma^{\mathrm{i}}_{\mathrm{cf,cr\,k;0.05}} = 0.150^2 \cdot 9.01 = 0.203 \text{ MN}$$

The load carried by the fibres in the crack can be determined according to (4.7) as follows

$$F_{\mathrm{f}} = A_{\mathrm{c}} \cdot \sigma_{\mathrm{cf}} = 0.150^2 \cdot 6.03 = 0.136 \text{ MN}$$

$$\text{with} \quad \sigma_{\mathrm{cf}} = \sigma_{\mathrm{cf0k;0.05}} \cdot \left(2 \cdot \sqrt{\frac{w_{\mathrm{k}}}{w_0}} - \frac{w_{\mathrm{k}}}{w_0}\right) = 6.03 \cdot \left(2 \cdot \sqrt{\frac{0.10}{0.106}} - \frac{0{,}10}{0.106}\right) = 6.03 \text{ N/mm}^2$$

For the crack width $w_{\mathrm{k}} = 0.10$ mm, the average bond stress between matrix and bar reinforcement can be determined for approximately stabilised cracking according to fig. 5.2 to be about $\tau_{\mathrm{sm}} \approx 3.3 \cdot f_{\mathrm{ctm}} = 3.3 \cdot 8.5 = 28 \text{ N/mm}^2$.

Furthermore, the evaluation of equation (4.17) requires an assumption of the concrete strain on the crack surface after crack formation. If the relaxation of the concrete is neglected on the safe side, then ε^*_{shr} corresponds with the free shrinkage coefficient of the concrete. For the mixture M2Q this amounts to about $\varepsilon_{cs} = -1‰$.

With a soldity coefficient of 0.4 instead of 0.6 and with $d_s = 16$ mm equation (4.17) results in

$$A_s = \Omega \cdot \left(-\varepsilon^*_{shr} + \sqrt{\varepsilon^{*\,2}_{shr} + 2 \cdot \frac{(F - F_f) - 0.4 \cdot (F_{f,cr} - F_f)}{\Omega \cdot E_s}} \right)$$

$$= 0.0957 \cdot \left(0.001 + \sqrt{0.001^2 + 2 \cdot \frac{(0.500 - 0.136) - 0.4 \cdot (0.203 - 0.136)}{0.0957 \cdot 200{,}000}} \right) \cdot 10^4$$

$$= 6{,}72 \text{ cm}^2$$

with $\Omega = \frac{(F_{f,cr} - F_f) \cdot d_s}{4 \cdot w_k \cdot \tau_{sm}} = \frac{(0.203 - 0.136) \cdot 16}{4 \cdot 0.10 \cdot 28} = 0.0957 \text{ m}^2$

According to equation (4.10), the maximum crack spacing amounts to

$$s_{r,max} = \frac{(F_{f,cr} - F_f) \cdot d_s}{2 \cdot \tau_{sm} \cdot A_s} = \frac{(0.203 - 0.136) \cdot 16}{2 \cdot 28 \cdot 6.72} \cdot 10^4 = 28 \text{ mm}$$

It is still to be proven that the bar reinforcement is in the elastic range. The tensile force carried by the bar reinforcement arises to

$$F_s = F - F_f = 0.500 - 0.136 = 0.364 \text{ MN}$$

With a provided bar reinforcement consisting of $4 \times d_s = 16$ mm ($\hat{=} 8.04$ cm^2), the steel stress amounts to

$$\sigma_s = \frac{F_s}{A_s} = \frac{0.364}{8.04} \cdot 10^4 = 453 \text{ N/mm}^2 < f_{yk} = 500 \text{ N/mm}^2$$

In spite of the comparatively small crack width, the steel stress is already very high. Therefore, in most cases, the determining factor of designing the bar reinforcement under action of loading will not be the crack width control but the verification of the load-carrying capacity in the ultimate limit state.

L2: The UHPC Tensile Member is Reinforced only with Rebars

In order to clarify the influence of the fibres on the crack formation, the crack width shall be limited for the tensile member examined before only by bar reinforcement.

The cracking force of the plain concrete matrix amounts to:

$$F_{cr} = A_c \cdot f_{ctm} = 0.150^2 \cdot 8.5 = 0{,}191 \text{ MN}$$

The remaining parameters can be taken from example L1. The possible degradation of bond conditions between matrix and bar reinforcement when omitting the fibres is neglected here.

Hence, the required bar reinforcement for the limitation of crack width amounts to

$$A_s = \Omega' \cdot \left(-\varepsilon_{shr}^* + \sqrt{\varepsilon_{shr}^{*\,2} + 2 \cdot \frac{F - 0.4 \cdot F_{cr}}{\Omega' \cdot E_s}} \right)$$

$$= 0.2729 \cdot \left(0.001 + \sqrt{0.001^2 + 2 \cdot \frac{0.500 - 0.4 \cdot 191}{0.2729 \cdot 200{,}000}} \right) \cdot 10^4 = 13.82 \text{ cm}^2$$

with $\Omega' = \frac{F_{cr} \cdot d_s}{4 \cdot w_k \cdot \tau_{sm}} = \frac{0.191 \cdot 16}{4 \cdot 0.10 \cdot 28} = 0.2729 \text{ m}^2$

The maximum crack spacing is

$$s_{r,max} = \frac{F_{cr} \cdot d_s}{2 \cdot \tau_{sm} \cdot A_s} = \frac{0.191 \cdot 16}{2 \cdot 28 \cdot 13.82} \cdot 10^4 = 40 \text{ mm}$$

With a provided bar reinforcement consisting of $8 \times d_s = 16$ mm ($\hat{=} 16.08 \text{ cm}^2$), the steel stress amounts to

$$\sigma_s = \frac{F_s}{A_s} = \frac{0.500}{16.08} \cdot 10^4 = 311 \text{ N/mm}^2 < f_{yk} = 500 \text{ N/mm}^2$$

The bar reinforcement ratio results for example L1 with $\rho_f = 0.9\,\%$ in $\rho_s = 3.0\,\%$ and for example L2 in $\rho_s = 6.1\,\%$. In this way, a reinforcement configuration optimised with regard to economic efficiency can be found for each structural element.

6 Summary

In [Leu07] a mechanical model is developed, which combines the mechanical relationships of the crack formation of reinforced concrete and the stress-crack opening-behaviour of the fibre-reinforced concrete considering the equilibrium of internal and external forces and the compatibility of deformations. The relationships relevant for the calculation of crack width are summarised and documented in the present paper.

During the process of crack formation, the phase of the single cracking, the state of stabilised cracking, and the phase of progressive crack formation are distinguished. The derived mechanical relationships permit also the consideration of the influence of shrinking on the crack formation.

By transforming and simplifying the quite complex relationships a design procedure for practical use is derived, that allows to determine directly the bar reinforcement required for the limitation of crack width. The use of this procedure demands only the knowledge of the fibre efficiency of a fibre-reinforced concrete mixture. Because of several influences that are not investigated sufficiently so far, the fibre efficiency can only be determined experimentally. Centric tensile tests on notched specimens are most appropriate for this.

Based on examples, the application of the proposed design procedure is illustrated and explained. Even with comparatively low fibre efficiencies a substantial improvement can be obtained compared to reinforced concrete. Therefore, under action of loading in most cases

instead of the crack width control the verification of the load-carrying capacity in the ultimate limit state will be the determining factor.

As experimental and theoretical investigations in [Leu07] show, a satisfying behaviour of UHPC in tension can be targeted by sufficiently designed bar reinforcement and without uneconomically high fibre contents. The secure limitation of crack width to definite less than 0.1 mm ensures at the same time the durability under unfavourable expositions.

The mechanical relationships derived in the present paper form in [Leu07] also the basis for the determination of the load-deformation-behaviour of a UHPC tensile member with combined reinforcement. Considering the variability of the material and geometrical characteristics a model is developed, where also statistical parameters, like e.g. the scatter of fibre distribution, are integrated. Thereby, a fictitious UHPC tensile member is divided into a finite number of elements of discrete length. These elements are the so-called crack elements. They represent the fibre distribution and the spectrum of the possible crack spacings at the state of stabilised cracking. By incremental load increase, the crack formation in the phase of progressive crack formation is simulated for each element and thus for each load step the frequency distribution of the crack spacings, of the crack widths, as well as the average tensile strain of the entire structural element are received. In this way, beside the process of crack formation also the load-deformation-behaviour of an UHPC tensile member with combined reinforcement can be reproduced consistently.

Literature

[AFGC02] Association Française de Génie Civil (AFGC)/Service d'études techniques des routes et autoroutes (SETRA): „Bétons fibrés à ultra-hautes performances", Recommandations provisoires, Janvier 2002.

[Bal99] *Balázs, G. L.* und *Kovács, I.*: „Concrete Members with Traditional Reinforcement and Fibers", in: Proceedings of the fib Symposium 1999, Vol. 1, Prague, 1999, 247-252.

[Beh96] *Behloul, M.*: „Les micro-bétons renforcés de fibres", in: De l'éprouvette aux structures, XIVèmes Journées de l'AUGC, Clermont-Ferrand, Prix Jeunes Chercheurs „René Houpert", 1996.

[Brü05] *Brühwiler, E.*; *Denarié, E.* und *Putallaz, J.-Chr.*: „Instandsetzung einer Betonbrücke mit ultrahochleistungsfähigem Faserfeinkornbeton (UHLFB)", *Beton- und Stahlbetonbau 100*, Heft 9, 2005, 822-827.

[Cha04] *Charron, J.-P.*; *Denarié, E.* und *Brühwiler, E.*: „Permeability of Ultra-High Performance Fibre Reinforced Concrete under high stresses", in: RILEM Symposium, Advances in Concrete Through Science and Engineering, Evanston, USA, March 2004, CD-ROM.

[DAfStb08] Deutscher Ausschuss für Stahlbeton (DAfStb): „Sachstandsbericht Ultrahochfester Beton", 1. Auflage 2008, Beuth Verlag GmbH, Berlin.

[DIN01] DIN 1045-1: „Tragwerke aus Beton, Stahlbeton und Spannbeton; Teil 1: Bemessung und Konstruktion", Normenausschuss Bauwesen (NABau) im DIN Deutsches Institut für Normung e. V., Berlin, Juli 2001.

[Feh05] *Fehling, E.*; *Schmidt, M.*; *Teichmann, Th.*; *Bunje, K.*; *Bornemann, R.* und *Middendorf, B.*: „Entwicklung, Dauerhaftigkeit und Berechnung Ultra-Hochfester Betone (UHPC)“, Forschungsbericht DFG FE 497/1-1, Schriftenreihe Baustoffe und Massivbau, Heft 1, Universität Kassel, 2005.

[Hab05] *Habel, K.*; *Denarié, E.* und *Brühwiler, E.*: „Bauteile aus ultrahochleistungsfähigem Faserbeton (UHPFRC) und traditionellem Stahlbeton“, *Beton- und Stahlbetonbau 100*, Heft 2, 2005, 124-131.

[Hab07] *Habel, K.*; *Denarié, E.* und *Brühwiler, E.*: „Experimental Investigation of Composite Ultra-High-Performance Fiber-Reinforced Concrete and Conventional Concrete Members“, *ACI Structural Journal*, Vol. 104, No. 1, January 2007.

[Hil76] *Hillerborg, A.*; *Modéer, M.* und *Petersson, P.-E.*: „Analysis of crack formation and crack growth in concrete by means of fracture mechanics and finite elements“, *Cement and Concrete Research*, Vol. 6, No. 6, 1976, 773-782.

[Jun06] *Jungwirth, J.*: „Zum Zugtragverhalten von zugbeanspruchten Bauteilen aus Ultra-Hochleistungs-Faserbeton“, Thèse N° 3429, Faculté Environnement Naturel, Architectural et Construit, École Polytechnique Fédérale de Lausanne, 2006.

[Ma03] *Ma, J.*; *Schneider, H.* und *Wu, Z.*: „Bruchmechanische Kenngrößen von UHFB“, in: Innovationen im Bauwesen: Ultrahochfester Beton (Hrsg.: *König, G.*; *Holschemacher, K.* und *Dehn, F.*), Bauwerk Verlag, Berlin, 2003, 121-130.

[Mar06] *Markovic, I.*: „High-Performance Hybrid-Fibre Concrete – Development and Utilisation“, Dissertation, TU Delft, 2006.

[Leu07] *Leutbecher, T.*: „Rissbildung und Zugtragverhalten von mit Stabstahl und Fasern bewehrtem Ultrahochfesten Beton (UHPC)“, Dissertation, Universität Kassel, 2007. http://www.uni-kassel.de/fb14/massivbau/DissLeutbecher.pdf

[Li92] *Li, V. C.* und *Leung, Ch. K. Y.*: „Steady-State and Multiple Cracking of Short Random Fiber Composites“, *Journal of Engineering Mechanics*, Vol. 188, No. 11, November 1992, 2246-2264.

[Pfy01] *Pfyl, Th.* und *Marti, P.*: „Versuche an stahlfaserverstärkten Stahlbetonelementen“, Institut für Baustatik und Konstruktion, ETH Zürich, Juli 2001.

[Pfy03] *Pfyl, Th.*: „Tragverhalten von Stahlfaserbeton“, Dissertation ETH Nr. 15005, ETH Zürich, 2003.

[Rei05] *Reinhardt, H.-W.*: „Beton“, in: Beton-Kalender 2005, Teil 2: Fertigteile, Tunnelbauwerke (Hrsg.: *Bergmeister, K.* und *Wörner, J.-D.*), Ernst & Sohn, Berlin, 2005, 1-141.

[Sch06] *Schumacher, P.*: „Rotation Capacity of Self-Compacting Steel Fiber Reinforced Concrete“, Dissertation, TU Delft, 2006.

[Voo03] *Voo*, J. Y. L. und Foster, S. J.: „Variable Engagement Model for Fibre Reinforced Concrete in Tension“, Uniciv Report No. R-420, The University of New South Wales, Sydney 2052, Australia, June 2003.

[Win98] *Winterberg, R.*: „Untersuchung zum Reißverhalten von Stahlfaserbeton und stahlfaserverstärktem Stahlbeton“, Dissertation, Institut für Konstruktiven Ingenieurbau, Ruhr-Universität Bochum, 1998.